Suporting Information

Sequentially solution-processed, nanostructured polymer photovoltaics using selective solvents

Do Hwan Kim,[1,3] Jianguo Mei,[1] Alexander L. Ayzner,[1,2] Kristin Schmidt,[2] Gaurav Giri,[1] Anthony L. Appleton,[1] Michael F. Toney,[2] Zhenan Bao[1,*]

[1] *Department of Chemical Engineering, Stanford University, 381 North-south Mall, Stanford, California 94305-5025, United States.*

[2] *Stanford Synchrotron Radiation Lightsource, SLAC National Accelerator Laboratory, Menlo Park, CA 94025, USA*

[3] *Department of Organic Materials and Fiber Engineering, Soongsil University, Seoul, 156-743, Korea*
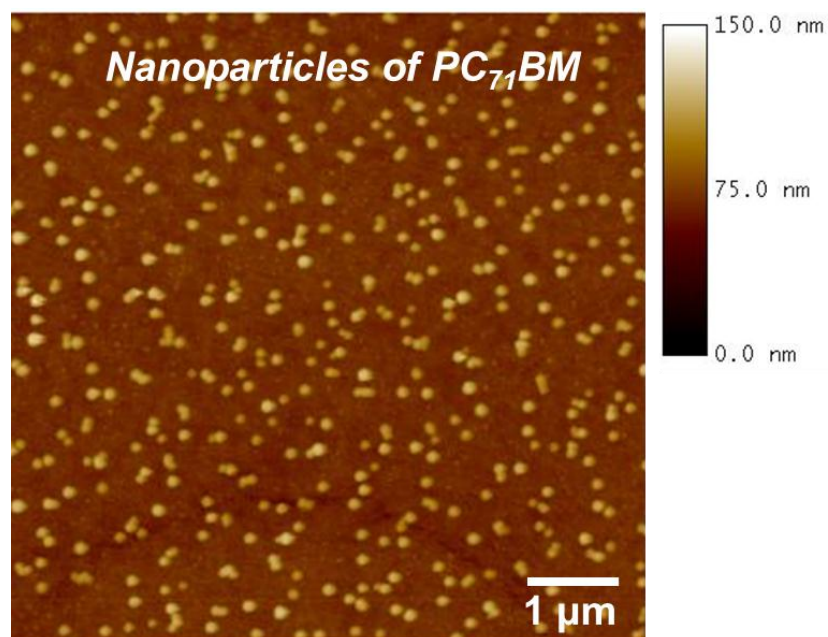
Figure S1. AFM image of PII2T-C10C8/$PC_{71}BM$ film after sequential processing of $PC_{71}BM$ layer derived from dichloromethane (DCM).
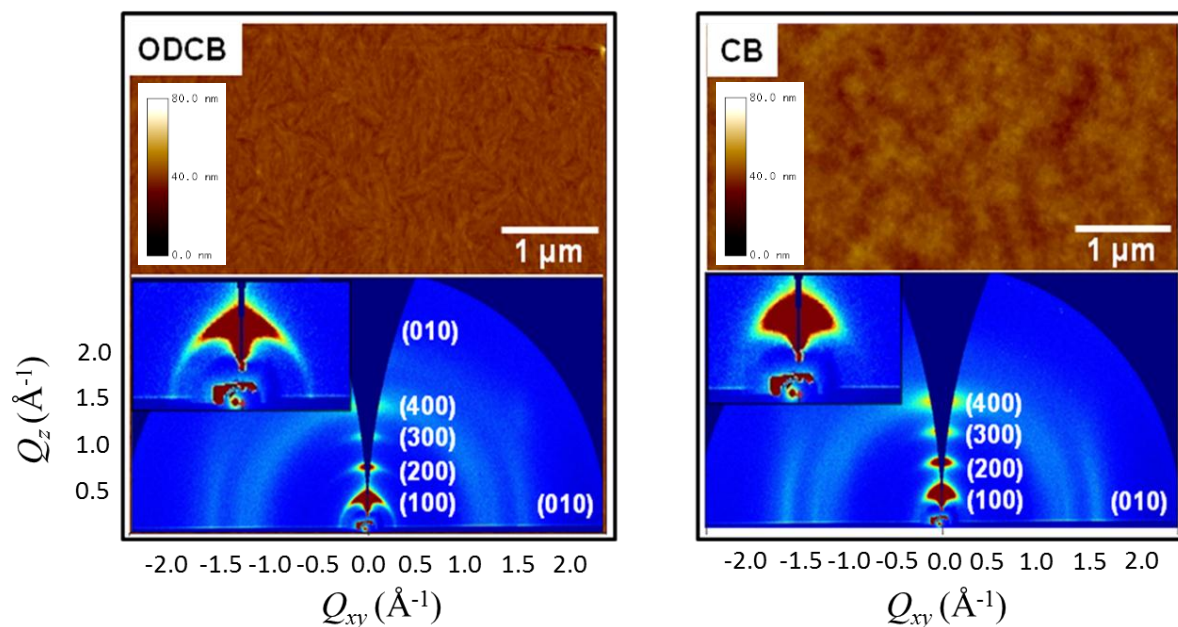
Figure S2. AFM topographs and GIXD patterns of neat PII2T-C10C8 films swollen by pure solvents and then annealed at 100 ^{o}C in glove box.

Given that the GIXD pattern of the ODCB-treated film shows a more isotropic crystallite orientation distribution, it is possible that the polymer film exposed to ODCB undergoes a greater degree of dissolution and immediate re-deposition onto the remaining film than when CB is used. This will likely lead to loss of memory of the substrate interaction, which primarily induces the strong edge-on orientation of the as-cast polymer film; therefore, a film with less preferential polymer orientation results following ODCB exposure.
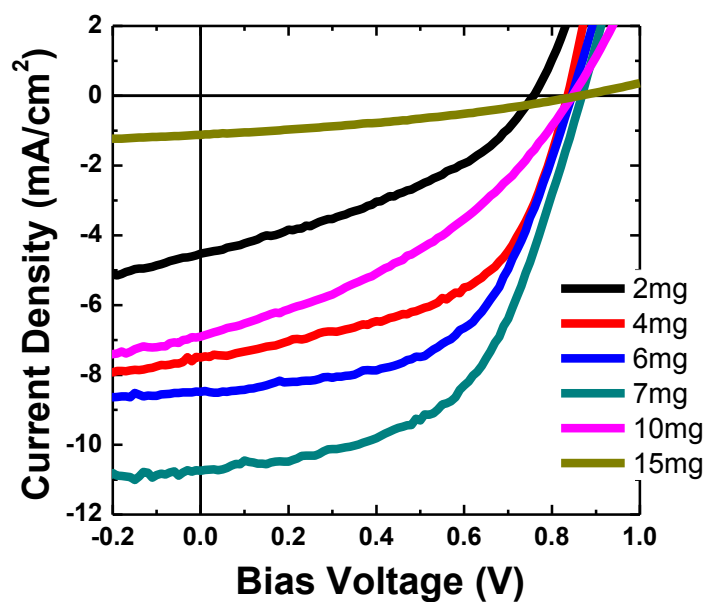

Figure S3. Current-voltage characteristics of PII2T-C10C8/PC$_{71}$BM SHJ solar cells as a function of donor concentration (deposited from ODCB).

Table S1. Performance parameters of SHJ solar cell as a function of PII2T-C10C8 concentration (deposited from ODCB).

| Polymer (conc.)	J_{SC} (mA/cm^2)	V_{OC} (V)	FF	PCE (%)
2mg (24nm)	-4.53	0.755	0.38	1.29
4mg (72nm)	-7.50	0.835	0.53	3.34
6mg (105nm)	-8.48	0.845	0.56	4.02
7mg (126nm)	-10.70	0.865	0.54	5.01
10mg (162nm)	-6.90	0.845	0.38	2.21
15mg (228nm)	-1.12	0.865	0.34	0.33
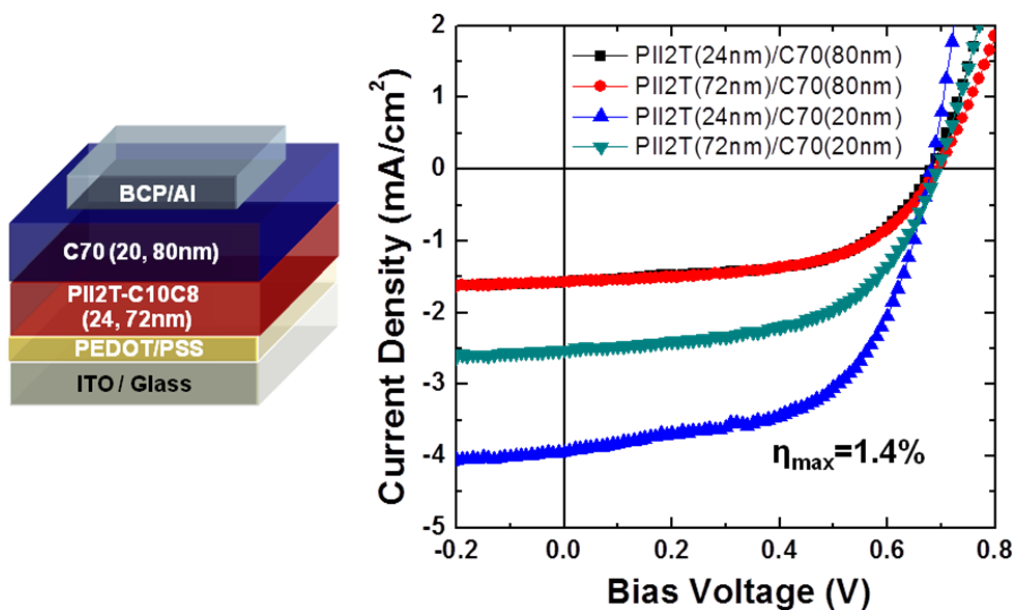
Figure S4. Current-voltage characteristic of PII2T-C10C8/C$_{70}$ planar heterojunction solar cells as a function of donor and C$_{70}$ thickness.
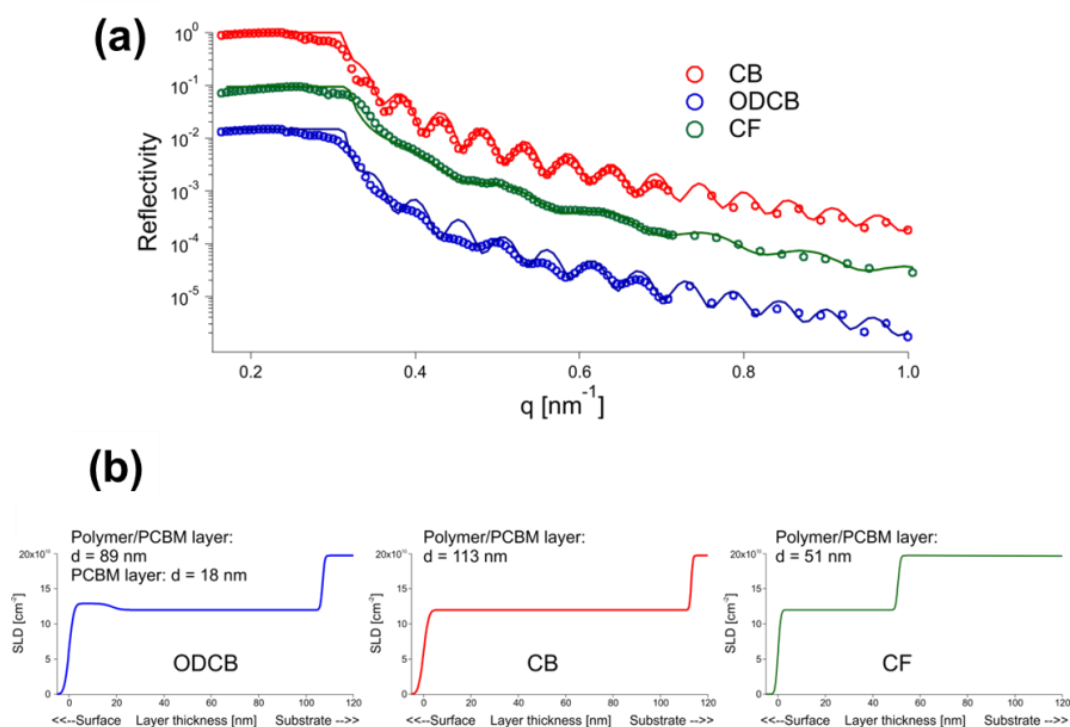
Figure S5 (a) X-ray reflectometry profiles with calculated models of PII2T-C10C8/PC$_{71}$BM SHJ films as a function of solvent. (b) SLD profiles of each film as determined from the fitting.

In order to further investigate the changes that are induced by the solvent used to spin-coat the fullerene and to measure the vertical electron density profiles, we have used X-ray reflectivity (XRR) measurements (Figure S5 and S6). In particular, we expect that whether fullerenes form a distinct overlayer on top of the polymer layer or whether the end result is a fully intermixed layer can be assessed by modeling XRR data. We also note that for all the films except for when ODCB was used, XRR data was fit well with a single layer model. However, in the ODCB case, the homogenous layer fit did not capture the Kiessing fringes well, so we attempted to use a bilayer model for further fitting. We find that neither model captures the data perfectly. It is likely that the vertical concentration profile in this case has a nontrivial functional form that is difficult to capture with a simple electron density model.
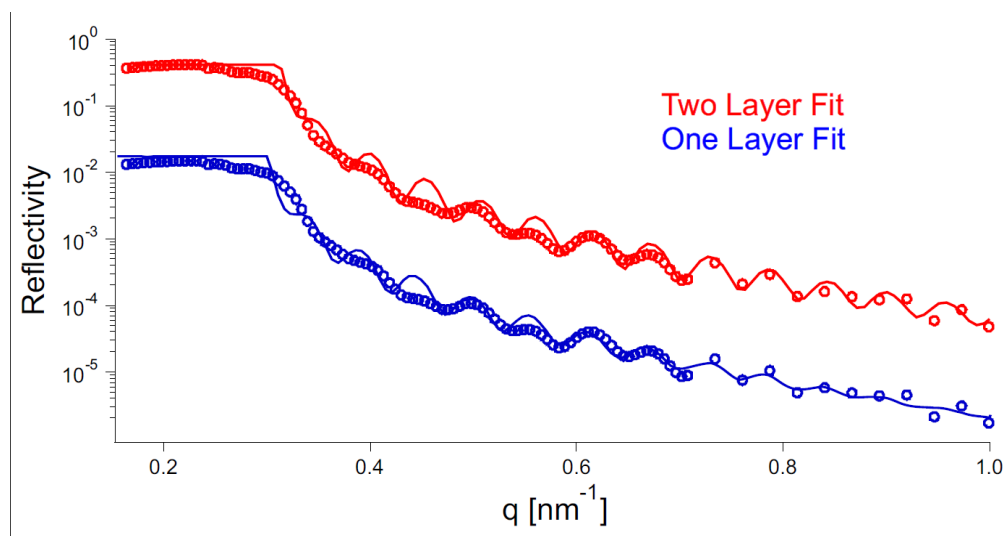
Figure S6. X-ray reflectometry profiles with calculated models of PII2T-C10C8/PC$_{71}$BM SHJ films fabricated by ODCB processing solvent